

# Axons Degenerate in the Absence of Mitochondria in *C. elegans*

Randi L. Rawson,<sup>1</sup> Lung Yam,<sup>2</sup> Robby M. Weimer,<sup>1,4</sup>  
Eric G. Bend,<sup>1</sup> Erika Hartwig,<sup>3</sup> H. Robert Horvitz,<sup>3</sup>  
Scott G. Clark,<sup>2,5</sup> and Erik M. Jorgensen<sup>1,\*</sup>

<sup>1</sup>Department of Biology and Howard Hughes Medical Institute, University of Utah, Salt Lake City, UT 84112-0840, USA

<sup>2</sup>Molecular Neurobiology Program, Department of Pharmacology, Skirball Institute, NYU School of Medicine, New York, NY 10016, USA

<sup>3</sup>Howard Hughes Medical Institute and Department of Biology, Massachusetts Institute of Technology, Cambridge, MA 02139, USA

## Summary

Many neurodegenerative disorders are associated with mitochondrial defects [1–3]. Mitochondria can play an active role in degeneration by releasing reactive oxygen species and apoptotic factors [4–7]. Alternatively, mitochondria can protect axons from stress and insults, for example by buffering calcium [8]. Recent studies manipulating mitochondria lend support to both of these models [9–13]. Here, we identify a *C. elegans* mutant, *ric-7*, in which mitochondria are unable to exit the neuron cell bodies, similar to the kinesin-1/*unc-116* mutant. When axons lacking mitochondria are cut with a laser, they rapidly degenerate. Some neurons even spontaneously degenerate in *ric-7* mutants. Degeneration can be suppressed by forcing mitochondria into the axons of the mutants. The protective effect of mitochondria is also observed in the wild-type: a majority of axon fragments containing a mitochondrion survive axotomy, whereas those lacking mitochondria degenerate. Thus, mitochondria are not required for axon degeneration and serve a protective role in *C. elegans* axons.

## Results

### *ric-7* Mutants Have Impaired Neurotransmission

We identified a novel gene, *ric-7* (resistant to inhibitors of cholinesterase), that is essential for mitochondrial localization in axons. Alleles were isolated in unrelated genetic screens either for mutants with neurotransmission defects or for mutants with abnormal axon morphology. The *ric-7* locus was identified by positional cloning and was also described by Hao et al. [14]. Microinjection of cosmid F58E10 rescued *ric-7* mutants, and microinjection of PCR fragments localized the rescuing activity to an 18 kb sequence predicted to contain two open reading frames, F58E10.1 and F58E10.7 (Figure 1A). To determine which open reading frame represents the *ric-7* locus, we identified the molecular lesions associated with the three *ric-7* alleles. All alleles contain mutations in predicted exons of F58E10.1 (Figure 1B; Table S1 available online). The potential functions of RIC-7 were not obvious from the

sequence; the RIC-7 protein lacks conserved domains and has rapidly diverged even among nematodes (Figure S1A).

Both acetylcholine and  $\gamma$ -aminobutyric acid (GABA) neurotransmission are impaired in *ric-7* mutants. Wild-type animals become paralyzed and die upon exposure to the acetylcholinesterase inhibitor Aldicarb. Paralysis is due to a buildup of acetylcholine in the synaptic cleft; thus, animals with impaired acetylcholine release are slower to respond to the drug. *ric-7* mutants are resistant to the effects of Aldicarb [14] (Figure S1B). GABA neurotransmission is also disrupted in *ric-7* mutants. In *C. elegans* defecation is a programmed behavior that requires GABA release onto the enteric muscles [15, 16]. *ric-7(n2657)* animals are constipated due to the absence of enteric muscle contractions [14] (Figure S1C). Restoring *ric-7* exclusively to GABA neurons using the *unc-47* promoter rescues the mutant defecation phenotype [“RIC-7(+)”], demonstrating that RIC-7 acts cell autonomously. These results demonstrate that mutations in *ric-7* disrupt both GABA and acetylcholine neurotransmission, suggesting that *ric-7* is generally required for synaptic transmission in *C. elegans*.

In spite of defects in neurotransmission, *ric-7* mutants have normal presynaptic structures. The active zone protein RIM (UNC-10), the synaptic vesicle protein vesicular GABA transporter (vGAT/UNC-47), and the dense-core vesicle protein FLP-3 are normally distributed along axons (Figures S1G–S1I). Wild-type and mutant animals have a similar density of synaptic puncta in GABA motor neurons (Figures S1D and S1E). *ric-7* synapses also appear normal at the ultrastructural level; specifically, there is no alteration in synaptic vesicle number (Figures S1F and S1J). Consistent with the normal appearance of synapses, *ric-7* mutants exhibit normal synaptic activity as measured by electrophysiology [14].

### Mitochondria Are Absent in Axons of *ric-7* Mutants

A transcriptional reporter construct indicates that the *ric-7* gene is expressed in most neurons and head muscles (Figure S1K). A translational reporter construct (Figure S2A) suggests that RIC-7 can associate with mitochondria. RIC-7 tagged at the N terminus with red fluorescent protein (RFP::RIC-7) can rescue *ric-7* mutants when expressed on extra-chromosomal arrays, and fluorescence colocalizes with the mitochondrial marker Tom20::GFP (mito::GFP) (Figure 2A). Single-copy insertions were dim or not visible (Figure S2B).

To determine whether mitochondria are altered in *ric-7* mutants, we examined the distribution of GFP-tagged mitochondria in wild-type and mutant animals. In the wild-type, mitochondria are distributed along the entire axon. However, in *ric-7* mutants, mitochondria are located almost exclusively in the cell bodies (Figures 2B and 2C). Occasionally, one or two mitochondria can be seen in proximal axons on the ventral side, typically near the cell body, whereas the distal axons in the dorsal nerve cord are completely void of mitochondria in *ric-7* mutants (Figure S2C). This suggests that in the few cases where mitochondria are able to exit the cell body, they cannot make it far in the absence of RIC-7. This mitochondrial distribution closely resembles that of the strong hypomorphic allele of kinesin-1 *unc-116(rh24sb79)*. The other predominant kinesin in *C. elegans* motor neurons, kinesin-3/*unc-104*, is not

<sup>4</sup>Present address: Department of Biomedical Imaging, Genentech, 1 DNA Way, South San Francisco, CA 94080, USA

<sup>5</sup>Present address: Department of Biology, University of Nevada, Reno, NV 89557, USA

\*Correspondence: [jorgensen@biology.utah.edu](mailto:jorgensen@biology.utah.edu)

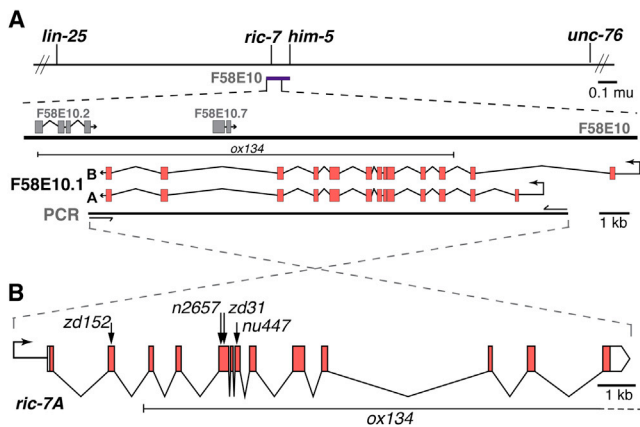


Figure 1. Cloning of *ric-7*

(A) The mutation *n2657* was mapped to the interval on chromosome V between *lin-25* and *unc-76*. Cosmid F58E10 (purple bar) spans 41 kb in this interval and rescued *ric-7* mutants as a transgene. Further experiments using PCR fragments indicated that rescuing activity was contained in an 18 kb fragment that contains two hypothetical genes, F58E10.1 and F58E10.7. Scale bar, 0.1 map unit (mu).

(B) All five *ric-7* alleles contain alterations in F58E10.1 exons (see Table S1). Arrows mark the locations of premature stops. *ox134* is a large deletion affecting three genes.

See also Figure S1 and Table S1.

required for trafficking of mitochondria out of the cell bodies (Figures 2B and 2D). Expressing N-terminally tagged RIC-7 (RFP::RIC-7) in *ric-7* mutants rescues the mitochondrial distribution in GABA neurons [Figure 2C, “RIC-7 (+)”].

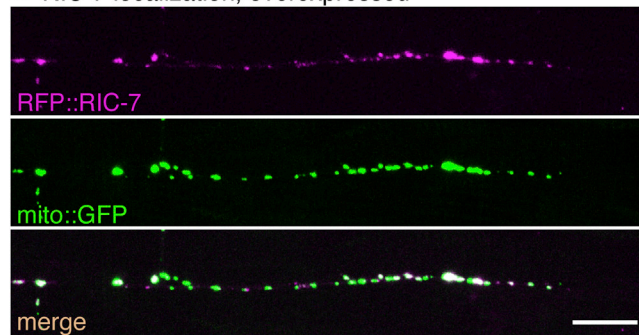
Mitochondrial distribution within other cell types, including muscle and hypodermis, is normal in *ric-7* mutants, indicating that *ric-7* does not have a general role in mitochondrial localization (Figures S2D and S2E). Other organelles such as synaptic vesicles and dense-core vesicles are normally distributed in *ric-7* mutant axons (Figures S1H and S1I). These data suggest that *ric-7* is specifically required for the localization of mitochondria in neurons.

#### Axon Degeneration Is Enhanced in *ric-7* Mutants

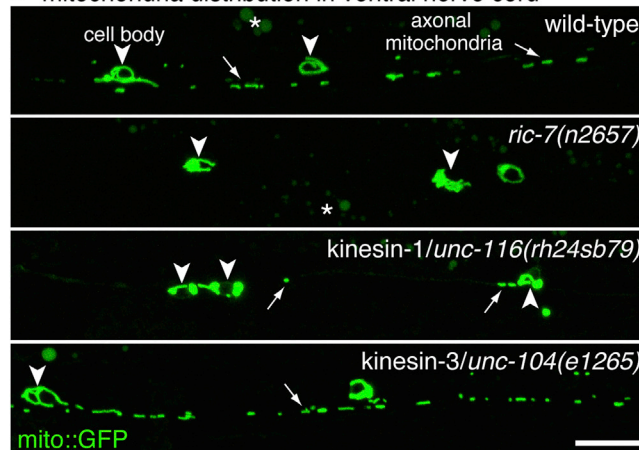
Axons from two neurons, PVQ and HSN, spontaneously degenerate in the absence of mitochondria. Mutations in *ric-7* were identified in an axon morphology screen because they had truncated PVQ axons in adult worms. However, the truncation is not due to an outgrowth defect; PVQ axons in *ric-7* mutants extend normally during embryogenesis and remain largely intact during the first three larval stages (Figures 3A and 3B; L1, L2, and L3, respectively). However, at the beginning of the fourth larval stage (L4), the axons begin to swell and degenerate (Figure 3C). By adulthood, most PVQ axons are truncated, typically near the vulva (Figure 3D). The proximal axon and cell body remain intact for the remaining life of the worm. The HSN axons, which grow out during early larval stages, degenerate in a similar fashion during early adulthood in *ric-7* mutants (Figures S3B–S3E).

Remarkably, the majority of axons in *ric-7* mutants remain stable throughout the life of the worm. Thus, *ric-7* mutants provide a tool to address whether mitochondria are required for axon degeneration. Severing the axon in a *ric-7* mutant provides an axon environment that is now completely removed from the influence of mitochondria. To determine the role of mitochondria in axon degeneration, GABA motor neuron

#### A RIC-7 localization, overexpressed



#### B mitochondria distribution in ventral nerve cord



#### C mitochondria number in ventral nerve cord

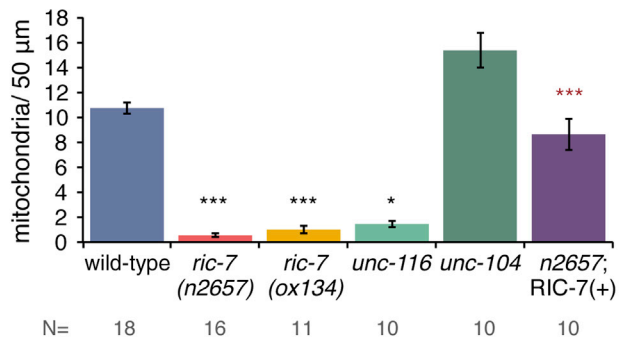


Figure 2. RIC-7 Colocalizes with Mitochondria and Is Required for Mitochondrial Distribution in Axons

(A) Tagged RIC-7 expressed in GABA neurons (*Punc-47::RFP::RIC-7, oxEx1598*) rescues *ric-7* mutants and colocalizes with mitochondria tagged with Tom20::GFP (mito::GFP). Worms were imaged with the dorsal nerve cord facing the objective. Scale bar, 10 μm. See also Figures S2A and S2B. (B) Mitochondria tagged with Tom20::GFP are trapped in the cell body and absent from axons in *ric-7* and *kinesin-1/unc-116* mutants but not *kinesin-3/unc-104* mutants. Arrowheads indicate cell bodies, and arrows point to axon mitochondria. Asterisks indicate gut autofluorescence. Worms were imaged with the ventral nerve cord facing the objective. Scale bar, 10 μm. See also Figures S2C and S2D.

(C) Average number of mitochondria per 50 μm in the ventral nerve cord of GABA motor neuron axons ± SEM. Mitochondrial distribution is rescued cell autonomously in axons when RFP::RIC-7 is expressed from an array [RIC-7(+), *oxEx1598*].  $p < 0.0001$ , Kruskal-Wallis test with Dunn’s multiple comparisons to the wild-type (black) and to *ric-7*(*n2657*) (red), \*\*\* $p < 0.001$ , \* $p < 0.05$ . The number of worms (N) is displayed below the graph. See also Figure S2.

**Mitochondria Suppress Degeneration**

3

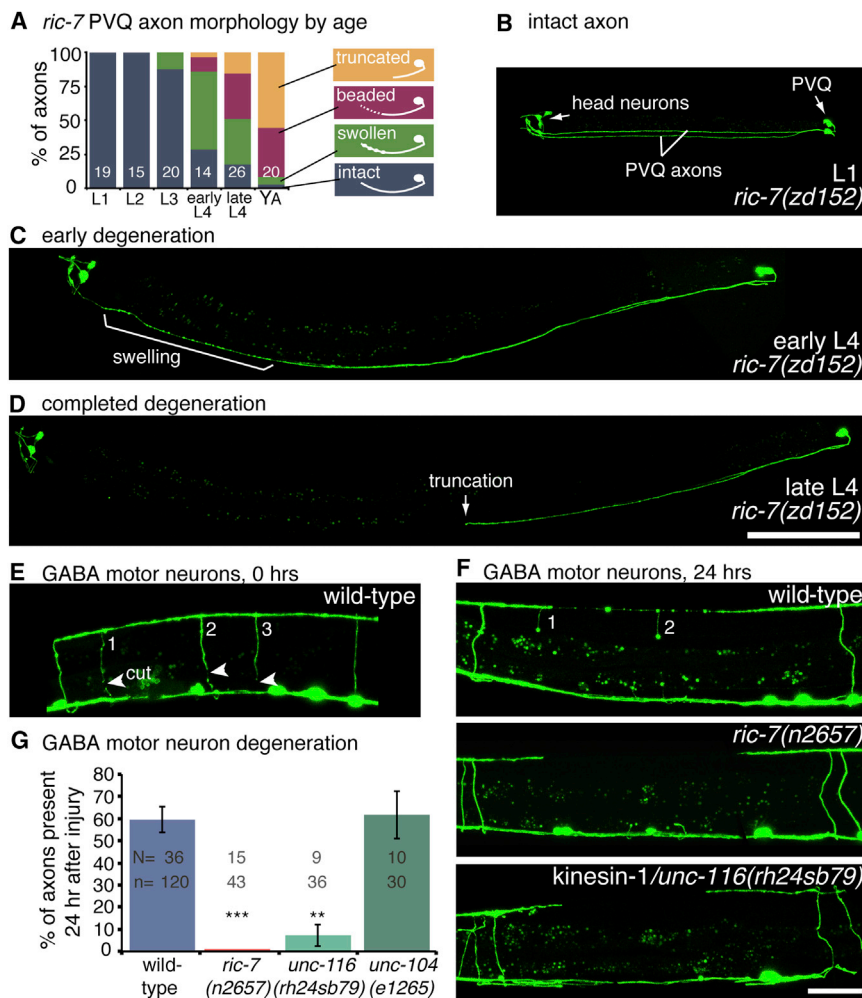


**Figure 3. Axon Degeneration Is Enhanced in the Absence of Mitochondria**

(A) PVQ axons spontaneously degenerate in *ric-7* mutants. The degenerating axons proceed through the following morphologies: swollen, beaded, and finally truncated. The percentage of axons with a given morphology is depicted for each life stage of *ric-7(zd152)*. The number of worms assayed is indicated. YA, young adult. (B) In the first larval stage, PVQ axons are intact in *ric-7(zd152)* mutants. GFP is expressed in PVQ and head neurons (ASH, ASI) under the *sra-6* promoter. The two PVQ cell bodies are in the tail; each extends an axon along the ventral nerve cord to the head. (C) During the fourth larval stage, the distal portion of the axon degenerates, beginning with swellings. (D) PVQ axons are typically truncated, frequently near the vulva, by the end of the fourth larval stage. The proximal half of the axons and the cell bodies remain intact. Scale bar, 100  $\mu$ m. See also [Figures S3A–S3E](#). (E) GABA motor neuron axons degenerate after laser axotomy. Arrowheads point to the cut sites in the image taken immediately after axotomy. There are three severed axons (numbered). (F) After 24 hr of recovery, worms were reimaged and the presence or absence of severed axons was scored. The wild-type panel is the same worm from (E). Two of the three axons exhibit swellings but are still present. Severed motor neuron axons completely degenerate in *ric-7* and kinesin-1/*unc-116* mutants. Scale bar, 25  $\mu$ m. (G) The average percentage of axons that are still present 24 hr after axotomy  $\pm$  SEM. More axons degenerate in mutants lacking mitochondria compared with the wild-type. The kinesin-3/*unc-104* mutant, which has mitochondria throughout its axons, degenerates at wild-type levels.  $p < 0.0001$ , Kruskal-Wallis test with Dunn's multiple comparisons to the wild-type, \*\*\* $p < 0.001$ , \*\* $p < 0.01$ . N, number of worms; n, number of axons. See also [Figures S3F–S3K](#). See also [Figure S3](#).

axons were cut using a laser in *ric-7* mutants and wild-type animals. Motor neuron axons cross from the ventral to the dorsal cord in single-axon commissures. The axons were visualized by expressing a soluble GFP under the *unc-47* (*vGAT*) promoter. Four to five commissures were severed in the posterior of L2 worms, typically three VD and one to two DD axons. The cell bodies were subsequently killed with a laser to prevent the regeneration of new axons, which would obscure the degenerating distal axons. After 24 hr of recovery, the worms were reimaged and the presence of commissures was scored. In wild-type worms, 58% of the GABA axons are present after 24 hr, whereas no axons remain in *ric-7* mutants ([Figures 3F and 3G](#)).

To determine whether additional cell types are hypersensitive to degeneration in *ric-7* mutants, we also performed axotomy on acetylcholine motor neurons and the ALA neuron. We expressed membrane-bound GFP under the *acr-5* promoter, which expresses in the acetylcholine DB motor neurons, ALA, and neurons in the head and tail ganglia. Two DB commissures were severed in each worm and then scored after 24 hr for their presence or absence. Only 11% of *ric-7* acetylcholine motor neuron axons remained after 24 hr, whereas 84% of wild-type axons were still present ([Figure S3F](#)). The ALA axon also displayed robust degeneration after injury in

*ric-7* mutants. The ALA neuron sends out two axons that run from the head to the tail on each side of the worm. Severed ALA axons are still present 24 hr after axotomy in the wild-type; however, in *ric-7* mutants severed axons completely degenerate ([Figures S3G and S3H](#)). Interestingly, injured axons are quite stable in wild-type *C. elegans*, which has been previously noted within regeneration studies [[17](#), [18](#)]. In all three cell types tested, *ric-7* mutants exhibited robust levels of axon degeneration.

**Mitochondrial Localization Mutants Have Enhanced Degeneration**

If the enhanced degeneration in *ric-7* mutants is due to the loss of mitochondria, then other mutants with aberrantly localized mitochondria should also have increased levels of axon degeneration. To test this we performed laser axotomy on kinesin-1 mutants, which also have a severe loss of mitochondria in their GABA motor neuron axons ([Figures 2B and 2C](#)). Similar to *ric-7*, the vast majority of injured axons degenerate in kinesin-1 mutants ([Figures 3F and 3G](#)). Kinesin-1 mutants could have increased degeneration due to their severe health impairments or to a general disruption in axon transport. However, mutants for kinesin-3/*unc-104*, which are equally unhealthy and deficient for key axon components such as

synaptic vesicles [19], have wild-type levels of degeneration (Figures 3F and 3G).

We also tested worms overexpressing a dominant-negative form of dynamin-related protein (DRP-1) in GABA neurons. DRP-1 is required for mitochondrial fission [20, 21], and neurons overexpressing a dominant-negative version, DRP-1(K40S), have long tubular mitochondria extending from the cell body into the proximal axons, but mitochondria numbers are reduced in the distal axons. When these axons lacking mitochondria are cut, they rapidly degenerate; only 23% of the axons remain after 24 hr (compared with 58% in the wild-type; Figures S3I–3K). Of these surviving axons, 70% contained visible escapee mitochondria when inspected. Thus, absence of mitochondria leads to an enhancement in axon degeneration in a variety of mutants.

### Mitochondria Prevent Axon Degeneration in Wild-Type Animals

To determine whether mitochondria mediate axon survival in healthy animals as well, we performed experiments on wild-type ALA axons. The ALA axon is long and has a naturally sparse distribution of mitochondria, with approximately one mitochondrion per 100  $\mu\text{m}$  ( $0.47 \pm 0.05$  mitochondria per 50  $\mu\text{m}$ ,  $N = 17$  L2 worms). To isolate axon segments that were void of mitochondria, the ALA axon was cut into multiple pieces. Because these axon segments receive a calcium influx through two lesion sites, they may be especially sensitive to the calcium buffering capacity of mitochondria. Each worm was imaged immediately after axotomy; roughly half of the fragments contained mitochondria (61%). Twenty-four hours later, axon segments were scored for survival; 72% of axon segments containing mitochondria survived, whereas only 26% of segments lacking visible mitochondria survived (Figures 4A–4C). Thus, the absence of mitochondria promotes degeneration in both mutant and wild-type axons.

Axons lacking mitochondria may be hypersensitive to degeneration due to a loss of metabolic support. To test whether mitochondrial metabolism is key for axon survival, mutants with electron transport chain defects were assayed for degeneration after axotomy. *nuo-1* encodes for a subunit of complex I and homozygous mutants arrest at the third larval stage [22]. Mutants lacking MEV-1, a subunit of complex II, are viable as homozygotes but are uncoordinated, slow growing, and have a shortened life span [23]. In spite of their mitochondrial dysfunction and health defects, these worms do not show an increase in axon degeneration after axotomy; instead, there are slightly more axons remaining compared with the wild-type (73% and 71%, respectively, of axons remain after 24 hr; Figure S4A). The electron transport chain mutants indicate that (1) mitochondrial dysfunction is insufficient to induce axon degeneration on its own and (2) energy levels are not likely to be the rate-limiting factor for axon preservation in *C. elegans*. In humans, nonlethal mutations affecting oxidative phosphorylation are rarely associated with neurodegeneration, suggesting that impaired mitochondrial bioenergetics do not reliably initiate degeneration [3]. In addition, some studies suggest that the glycolytic activity of a cell can promote survival during impaired oxidative phosphorylation [24–28].

### Restoring Mitochondria in *ric-7* Mutant Axons Suppresses Degeneration

Even though mutant and wild-type axons lacking mitochondria have enhanced degeneration, it still remains possible that

axon degeneration in *ric-7* mutants is caused by another defect, not noticed in our assays. If mitochondrial loss is responsible for the enhanced degeneration, then restoring mitochondria into *ric-7* deficient axons should suppress axon degeneration. To rescue mitochondrial localization in *ric-7* mutants, we constructed a chimeric transport protein that fuses Kinesin-1 (UNC-116) to the outer mitochondrial membrane protein Tom7 (encoded by *tomm-7*) (Figure 4D, Kinesin-Tom7). The proteins are separated by linkers and GFP. When the chimeric transport protein is expressed in GABA neurons, mitochondria are transported into the axons of *ric-7* mutants (Figures 4E and S4B). It is also notable that expression of the transport chimera also rescues GABA motor neuron function (Figure 4F). Restoring mitochondria to axons in *ric-7* mutants also fully suppresses the degeneration phenotype. Axon survival after axotomy is 52% in *ric-7* animals in which the Kinesin-Tom7 construct is expressed (compared with 58% in the wild-type and 0% in *ric-7*; Figures 4G and S4C). Expression of the transport chimera does not influence degeneration in the wild-type. Rescue by forced transport of mitochondria in the *ric-7* mutant demonstrates that the relevant cause of rapid axon degeneration and defective neurotransmission is the absence of mitochondria.

### Discussion

Recent studies suggest contradictory roles for mitochondria in axon degeneration. In some cases, mitochondria seem to prevent axon degeneration. For example, loss of mitochondria caused by knockdown of the kinesin adaptor *milton* led to degeneration of axons in the fly wing [11]. Similarly, disease-associated alleles of *mitofusin 2* in cultured dorsal root ganglia neurons disrupted the regular distribution of mitochondria in axons and was associated with degeneration [24].

In other cases, mitochondria seem to promote axon degeneration. For example, degeneration of neuromuscular junctions is caused by knockdown of alpha-spectrin in flies, and this degeneration is suppressed by mutations in the mitochondrial transport adaptor *miro* [10]. In another example, the degeneration of severed axons was prevented by blocking the mitochondrial permeability transition pore with the drug cyclosporin A [9]. Severed sciatic nerves were cultured in the absence of their neuronal cell bodies; thus, the drug is acting on mitochondria within the axon to prevent degeneration. These studies indicate that mitochondria promote axon degeneration in both a disease model and an injury-based model.

Our data demonstrate that mitochondria are not a necessary component of the degeneration process but rather are required for the protection of axons in *C. elegans*. In *ric-7* mutants, mitochondria never migrate into the axons. Some axons lacking mitochondria spontaneously degenerate in *ric-7* mutants, and axons that are intact rapidly degenerate after an injury. Other strains with disrupted mitochondrial localization, such as animals defective for mitochondrial transport (kinesin-1) or mitochondrial division [DRP-1(K40S)], also exhibit rapid degeneration after axotomy. Importantly, the absence of mitochondria in wild-type axons also causes degeneration, demonstrating that neurodegeneration is not due to secondary defects of the mutations, but rather is due to the absence of mitochondria. The protective role of mitochondria is underscored by their ability to rescue degeneration when they are forced into axons. Hauling mitochondria out of cell bodies in *ric-7* mutants using a chimeric transport protein

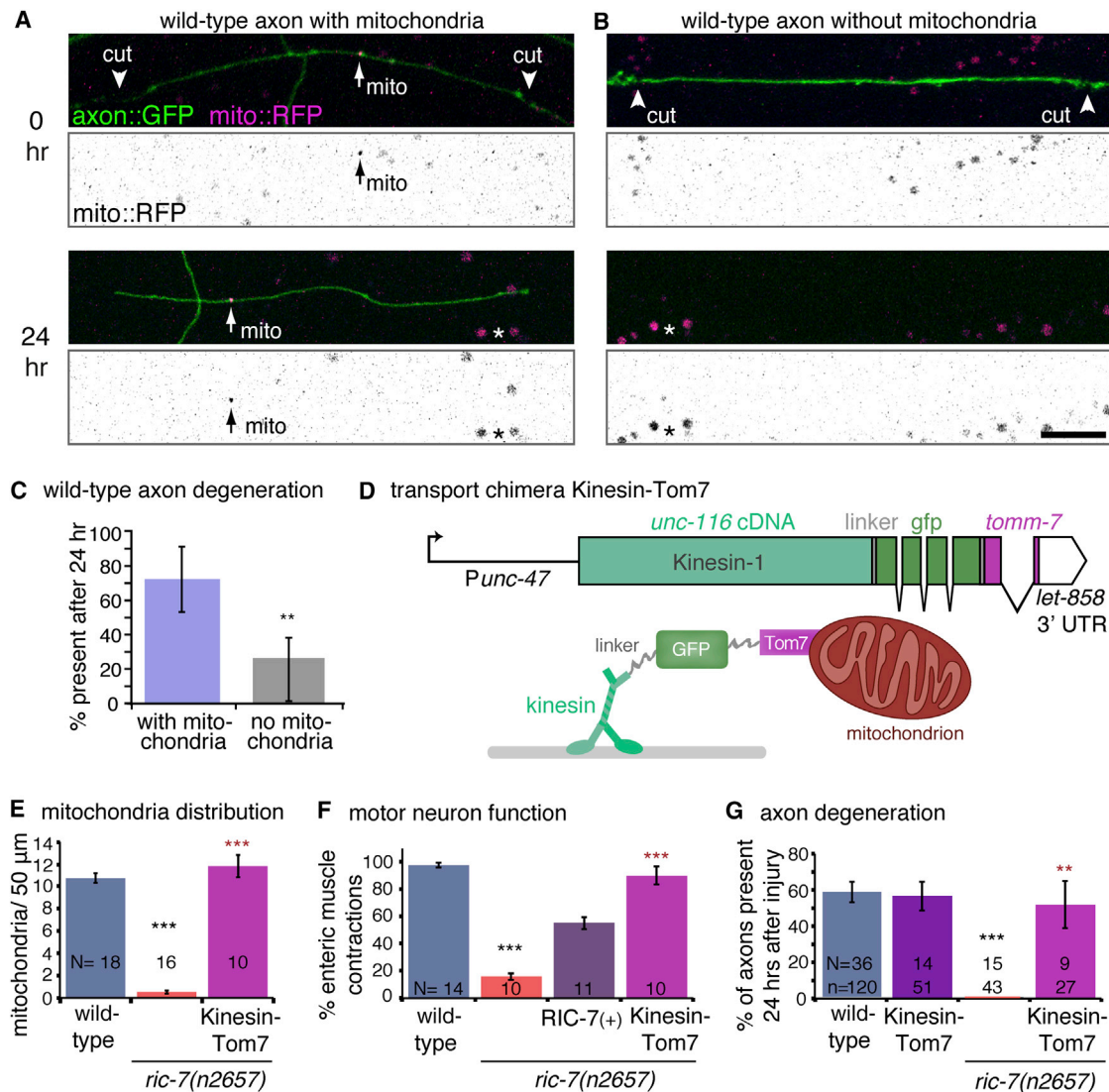


Figure 4. Mitochondria Mediate Axon Protection

(A and B) The presence of mitochondria protects axons from degeneration in a wild-type background. ALA axons are labeled by expressing membrane-bound GFP under the *acr-5* promoter (axon::GFP), and mitochondria are labeled by expressing mito::RFP under the *ida-1* promoter. ALA axons were cut by laser axotomy into multiple segments in wild-type worms that either contained (A) or lacked (B) mitochondria. Twenty-four hours after axotomy, the axon segment with a mitochondrion was still intact (below), whereas the segment without a mitochondrion had degenerated. The mito::RFP images have been inverted, and the contrast has been enhanced to increase the visibility of the mitochondria (arrows). Asterisks indicate gut autofluorescence. Scale bar, 10  $\mu$ m.

(C) Seventy-two percent of the axon fragments containing a mitochondrion were still present 24 hr later, whereas only 26% of axon fragments without mitochondria perished. Error bars represent the 95% confidence interval ( $p = 0.0028$ , two-tailed Fisher's exact test;  $N = 13$  worms and  $n = 48$  axon fragments).

(D) Top: a transport chimera construct was created by fusing the cDNA for *unc-116* (kinesin-1) to the *tomm-7* gene, which encodes for the outer mitochondrial membrane protein Tom7. GFP flanked by linkers was inserted between the motor and the mitochondrial protein. The construct was expressed in GABA neurons under the *unc-47* promoter. Bottom: a conceptual cartoon of the transport chimera protein.

(E) Expression of the transport chimera Kinesin-Tom7 restores mitochondria in *ric-7* mutant axons. N, number of worms. See also Figure S4B.

(F) The transport chimera suppresses the GABA neurotransmission defects in *ric-7* mutants. In *C. elegans* GABA release is required for enteric muscle contractions (emc) following posterior body muscle contractions (pboc). In *ric-7* mutants only 16% of pbocs are followed by an emc. This defect was rescued by expressing RIC-7(+) (*oxEx1598*[RFP::RIC-7]), or the transport chimera Kinesin-Tom7 in GABA neurons. N, number of worms.

(G) Restoring mitochondria to *ric-7* mutant axons (magenta bar) also suppressed degeneration of GABA motor neuron axons after injury. The transport chimera has no effect in a wild-type background (purple bar). The wild-type and *ric-7* data are the same as in Figure 3G. See also Figure S4C.

For (E)–(G),  $p < 0.0001$ , Kruskal-Wallis test with Dunn's multiple comparisons to the wild-type (black) and to *ric-7*(n2657) (red), \*\*\* $p < 0.001$ , \*\* $p < 0.01$ . N, number of worms; n, number of axons. See also Figure S4.

(Kinesin-Tom7) rescues both neurotransmission and axon degeneration in *ric-7* mutants.

Perhaps a more nuanced view of mitochondria is warranted; they are neither solely protective nor destructive, but rather

seem to play both Jekyll-and-Hyde roles in neurodegeneration. Previous data have demonstrated that mitochondria can promote or accelerate degeneration in certain disease states (reviewed in [3, 10]). Here, we show that mitochondria

are required for axon stability in *C. elegans*. The absence of mitochondria causes rapid degeneration of cut axons in both wild-type and mutant axons. These observations suggest two further conclusions. First, mitochondria are not required for degeneration. In other words, the swelling, beading, and engulfment processes are not directed by mitochondria but must lie within the molecular pathways of the axon itself and the surrounding cells. Second, mitochondria provide an active, protective role, somehow blocking the initiation of these processes.

#### Supplemental Information

Supplemental Information includes Supplemental Experimental Procedures, four figures, and one table and can be found with this article online at <http://dx.doi.org/10.1016/j.cub.2014.02.025>.

#### Acknowledgments

We thank Jamie White, Marc Hammarlund, and Holly Holman for critical review of the manuscript. We thank Mike Bastiani and Paola Nix for the use of their laser axotomy system. We are grateful to Villu Maricq and Dane Maxfield for the use of their Nikon spinning disc confocal. We thank the following people for providing reagents: Kim Schuske, Rob Hobson, Andrew Jones, Marc Hammarlund, Shaili Johri, Fred Horndli, Jean Louis Bessereau, and Gunther Höllopeter. The FLP-3::Venus strain was a gift from Ken Miller. The *unc-116(rh24sb79)* strain was a gift from Frank McNally. Some strains were provided by the CGC (NIH P40 OD010440). The *nu447* allele was a gift from Josh Kaplan, and we appreciate discussions before publication. This work was supported by NIH grant NS39397 to S.G.C. and NIH grant NS034307 and NSF grant IOS-0920069 to E.M.J.

Received: November 29, 2012

Revised: January 7, 2014

Accepted: February 11, 2014

Published: March 13, 2014

#### References

- Patten, D.A., Germain, M., Kelly, M.A., and Slack, R.S. (2010). Reactive oxygen species: stuck in the middle of neurodegeneration. *J. Alzheimers Dis.* 20 (Suppl 2), S357–S367.
- Chang, D.T.W., Rintoul, G.L., Pandipati, S., and Reynolds, I.J. (2006). Mutant huntingtin aggregates impair mitochondrial movement and trafficking in cortical neurons. *Neurobiol. Dis.* 22, 388–400.
- Schon, E.A., and Przedborski, S. (2011). Mitochondria: the next (neurode)generation. *Neuron* 70, 1033–1053.
- Alvarez, S., Moldovan, M., and Krarup, C. (2008). Acute energy restriction triggers Wallerian degeneration in mouse. *Exp. Neurol.* 212, 166–178.
- Lucius, R., and Sievers, J. (1996). Postnatal retinal ganglion cells in vitro: protection against reactive oxygen species (ROS)-induced axonal degeneration by cocultured astrocytes. *Brain Res.* 743, 56–62.
- Koeberle, P.D., and Ball, A.K. (1999). Nitric oxide synthase inhibition delays axonal degeneration and promotes the survival of axotomized retinal ganglion cells. *Exp. Neurol.* 158, 366–381.
- Shigenaga, M.K., Hagen, T.M., and Ames, B.N. (1994). Oxidative damage and mitochondrial decay in aging. *Proc. Natl. Acad. Sci. USA* 91, 10771–10778.
- Avery, M.A., Rooney, T.M., Pandya, J.D., Wishart, T.M., Gillingwater, T.H., Geddes, J.W., Sullivan, P.G., and Freeman, M.R. (2012). WldS prevents axon degeneration through increased mitochondrial flux and enhanced mitochondrial Ca<sup>2+</sup> buffering. *Curr. Biol.* 22, 596–600.
- Barrientos, S.A., Martinez, N.W., Yoo, S., Jara, J.S., Zamorano, S., Hetz, C., Twiss, J.L., Alvarez, J., and Court, F.A. (2011). Axonal degeneration is mediated by the mitochondrial permeability transition pore. *J. Neurosci.* 31, 966–978.
- Keller, L.C., Cheng, L., Locke, C.J., Müller, M., Fetter, R.D., and Davis, G.W. (2011). Glial-derived prodegenerative signaling in the *Drosophila* neuromuscular system. *Neuron* 72, 760–775.
- Fang, Y., Soares, L., Teng, X., Geary, M., and Bonini, N.M. (2012). A novel *Drosophila* model of nerve injury reveals an essential role of Nmnat in maintaining axonal integrity. *Curr. Biol.* 22, 590–595.
- Iijima-Ando, K., Sekiya, M., Maruko-Otake, A., Ohtake, Y., Suzuki, E., Lu, B., and Iijima, K.M. (2012). Loss of axonal mitochondria promotes tau-mediated neurodegeneration and Alzheimer's disease-related tau phosphorylation via PAR-1. *PLoS Genet.* 8, e1002918.
- Kitay, B.M., McCormack, R., Wang, Y., Tsoulfas, P., and Zhai, R.G. (2013). Mislocalization of neuronal mitochondria reveals regulation of Wallerian degeneration and NMNAT/WLD<sup>(S)</sup>-mediated axon protection independent of axonal mitochondria. *Hum. Mol. Genet.* 22, 1601–1614.
- Hao, Y., Hu, Z., Sieburth, D., and Kaplan, J.M. (2012). RIC-7 promotes neuropeptide secretion. *PLoS Genet.* 8, e1002464.
- Liu, D.W., and Thomas, J.H. (1994). Regulation of a periodic motor program in *C. elegans*. *J. Neurosci.* 14, 1953–1962.
- McIntire, S.L., Jorgensen, E., Kaplan, J., and Horvitz, H.R. (1993). The GABAergic nervous system of *Caenorhabditis elegans*. *Nature* 364, 337–341.
- Wu, Z., Ghosh-Roy, A., Yanik, M.F., Zhang, J.Z., Jin, Y., and Chisholm, A.D. (2007). *Caenorhabditis elegans* neuronal regeneration is influenced by life stage, ephrin signaling, and synaptic branching. *Proc. Natl. Acad. Sci. USA* 104, 15132–15137.
- Pinan-Lucarre, B., Gabel, C.V., Reina, C.P., Hulme, S.E., Shevkoplyas, S.S., Stone, R.D., Xue, J., Qiao, Y., Weisberg, S., Roodhouse, K., Sun, L., et al. (2012). The core apoptotic executioner proteins CED-3 and CED-4 promote initiation of neuronal regeneration in *Caenorhabditis elegans*. *PLoS Biol.* 10, e1001331.
- Hall, D.H., and Hedgecock, E.M. (1991). Kinesin-related gene *unc-104* is required for axonal transport of synaptic vesicles in *C. elegans*. *Cell* 65, 837–847.
- Otsuga, D., Keegan, B.R., Brisch, E., Thatcher, J.W., Hermann, G.J., Bleazard, W., and Shaw, J.M. (1998). The dynamin-related GTPase, Dnm1p, controls mitochondrial morphology in yeast. *J. Cell Biol.* 143, 333–349.
- Smirnova, E., Shurland, D.L., Ryazantsev, S.N., and van der Bliek, A.M. (1998). A human dynamin-related protein controls the distribution of mitochondria. *J. Cell Biol.* 143, 351–358.
- Tsang, W.Y., Sayles, L.C., Grad, L.I., Pilgrim, D.B., and Lemire, B.D. (2001). Mitochondrial respiratory chain deficiency in *Caenorhabditis elegans* results in developmental arrest and increased life span. *J. Biol. Chem.* 276, 32240–32246.
- Ishii, N., Fujii, M., Hartman, P.S., Tsuda, M., Yasuda, K., Senoo-Matsuda, N., Yanase, S., Ayusawa, D., and Suzuki, K. (1998). A mutation in succinate dehydrogenase cytochrome b causes oxidative stress and ageing in nematodes. *Nature* 394, 694–697.
- Misko, A.L., Sasaki, Y., Tuck, E., Milbrandt, J., and Baloh, R.H. (2012). Mitofusin2 mutations disrupt axonal mitochondrial positioning and promote axon degeneration. *J. Neurosci.* 32, 4145–4155.
- Calupca, M.A., Hendricks, G.M., Hardwick, J.C., and Parsons, R.L. (1999). Role of mitochondrial dysfunction in the Ca<sup>2+</sup>-induced decline of transmitter release at K<sup>+</sup>-depolarized motor neuron terminals. *J. Neurophysiol.* 81, 498–506.
- Winkler, B.S., Arnold, M.J., Brassell, M.A., and Puro, D.G. (2000). Energy metabolism in human retinal Müller cells. *Invest. Ophthalmol. Vis. Sci.* 41, 3183–3190.
- Tekkök, S.B., Brown, A.M., and Ransom, B.R. (2003). Axon function persists during anoxia in mammalian white matter. *J. Cereb. Blood Flow Metab.* 23, 1340–1347.
- Fünfschilling, U., Supplie, L.M., Mahad, D., Boretius, S., Saab, A.S., Edgar, J., Brinkmann, B.G., Kassmann, C.M., Tzvetanova, I.D., Möbius, W., Diaz, F., et al. (2012). Glycolytic oligodendrocytes maintain myelin and long-term axonal integrity. *Nature* 485, 517–521.

**Current Biology, Volume 24**

**Supplemental Information**

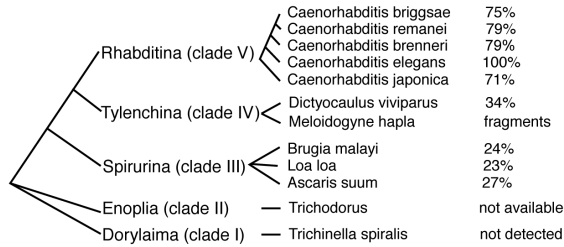
**Axons Degenerate in the Absence**

**of Mitochondria in *C. elegans***

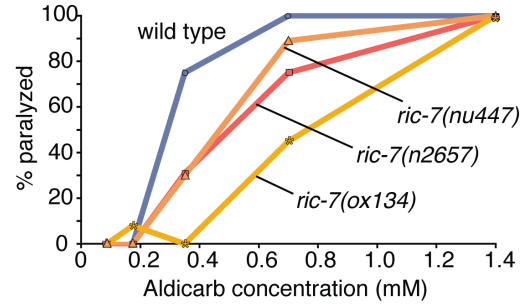
**Randi L. Rawson, Lung Yam, Robby M. Weimer, Eric G. Bend, Erika Hartweg, H. Robert Horvitz, Scott G. Clark, and Erik M. Jorgensen**

Figure S1

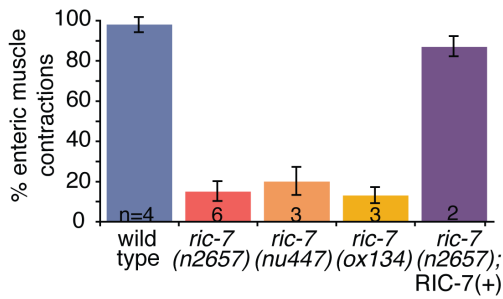
A % identity among RIC-7B orthologs



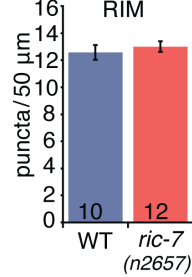
B Acetylcholine function



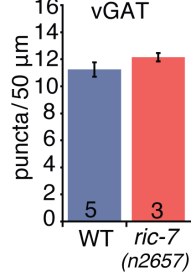
C GABA function



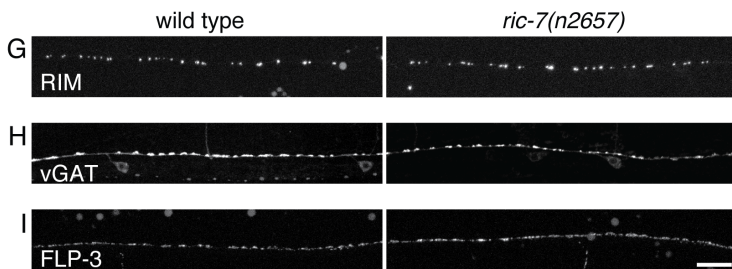
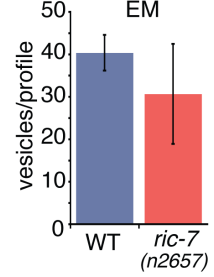
D



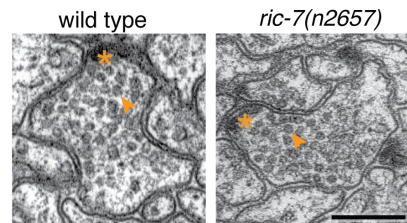
E



F



J synapse ultrastructure



K

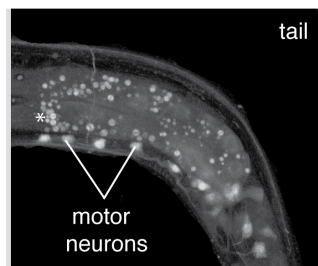
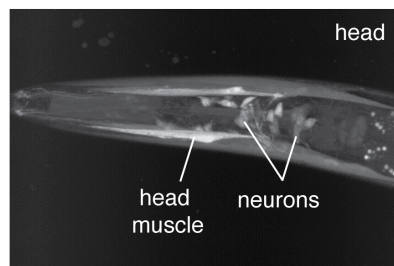
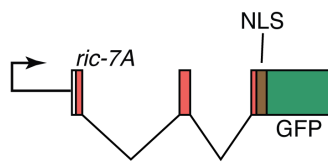


Figure S2

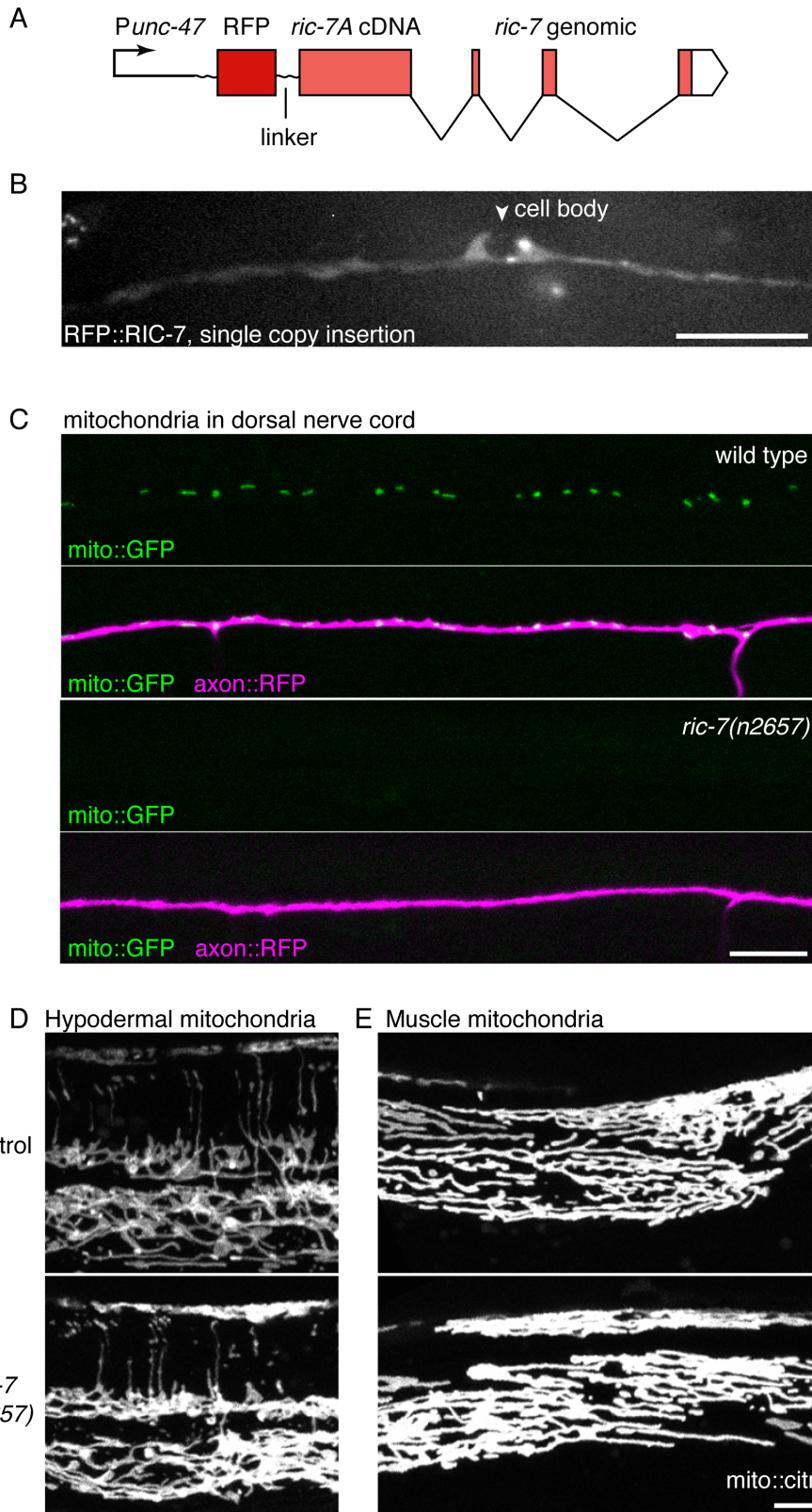
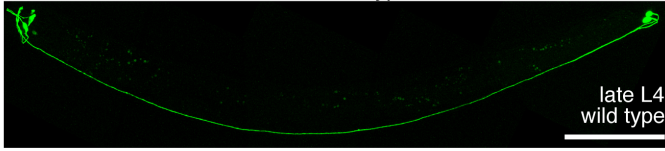
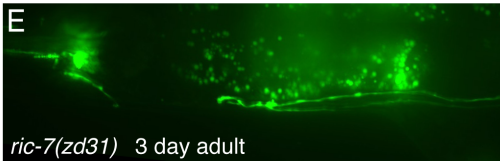
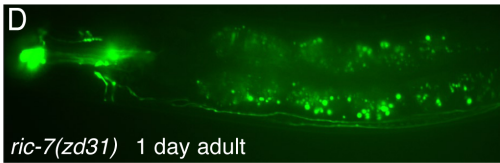
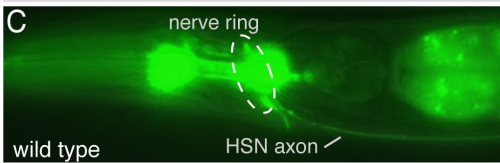
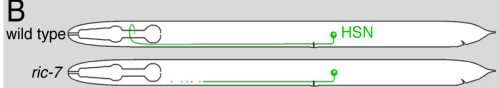


Figure S3

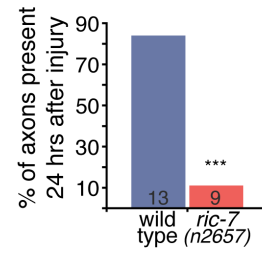
A PVQ axons remain intact in wild-type worms



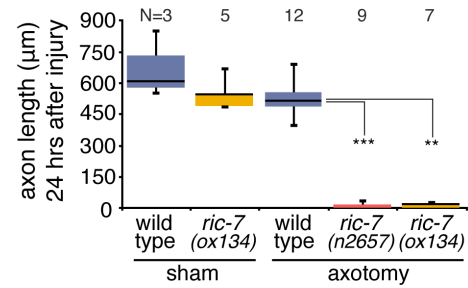
B HSN axons spontaneously degenerate in *ric-7* mutants



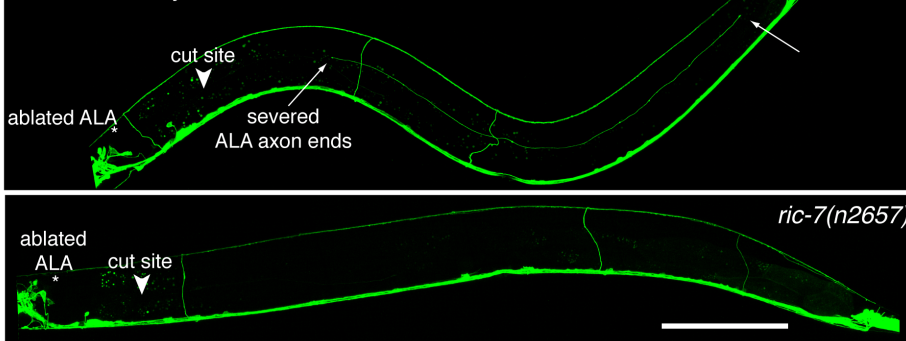
F ACh motor neuron degeneration



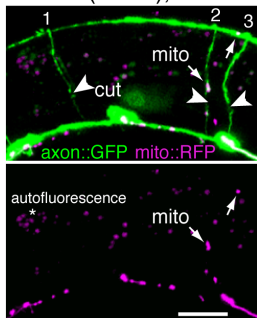
G ALA axon length



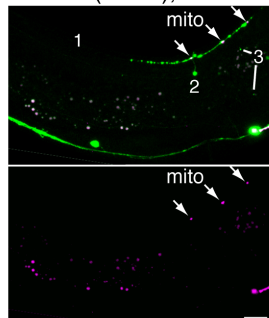
H ALA axotomy



I DRP-1(K40S), 0 hrs



J DRP-1(K40S), 24 hrs



K GABA motor neuron degeneration

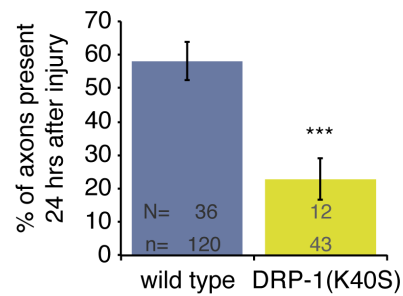
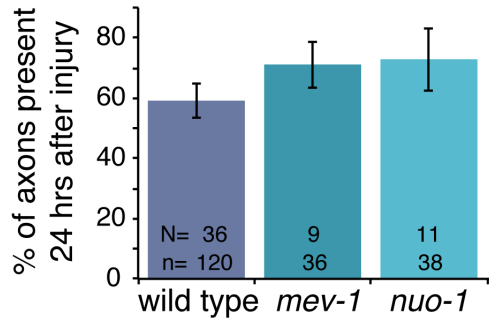
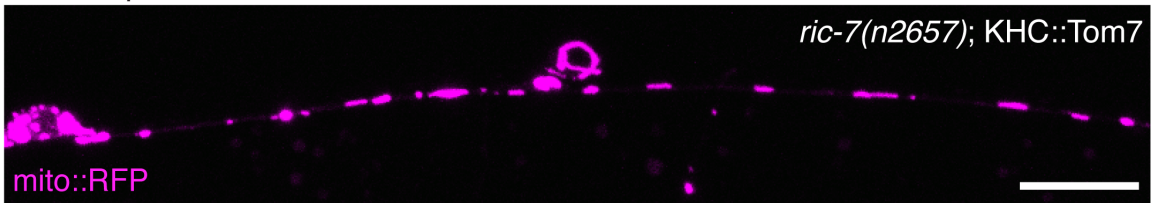


Figure S4

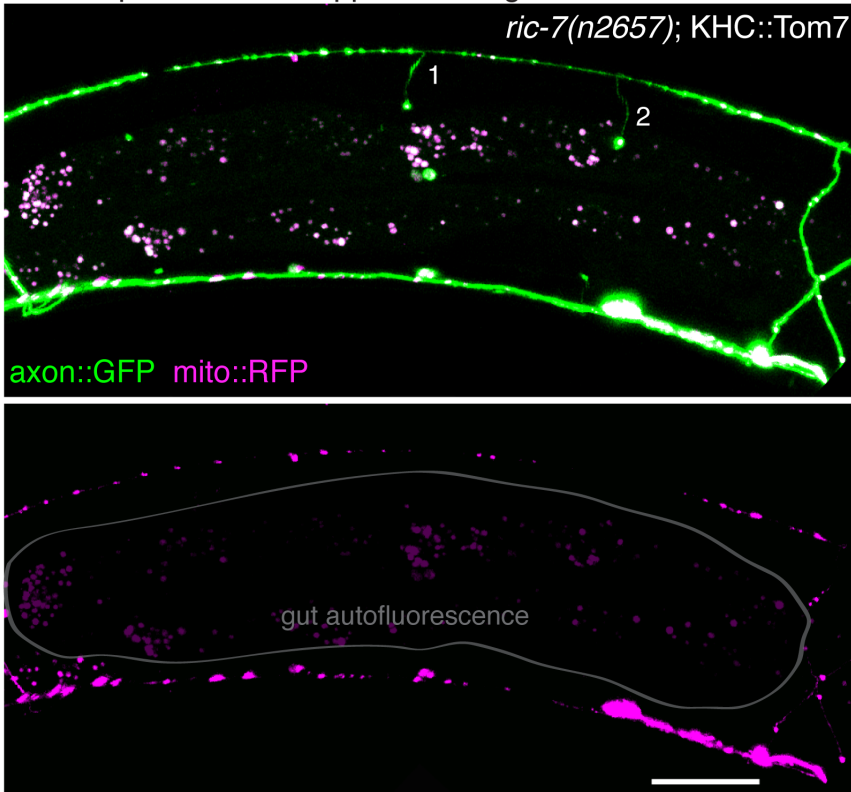
A mitochondria dysfunction



B transport chimera rescues mitochondria distribution



C transport chimera suppresses degeneration



## SUPPLEMENTAL FIGURE LEGENDS

**Figure S1. Characterization of *ric-7*, related to Figure 1.** (A) The phylogenetic tree of RIC-7B orthologs shows rapid divergence among nematodes. The RIC-7A isoform is present only in the Rhabditina clade. RIC-7 from *C. elegans* and *B. malayi* only share 23% identity; other mitochondrial proteins such as MIRO share 58% identity in these species. Orthologs of the RIC-7 isoforms were identified by performing BLAST searches of other nematode sequence data and were hand-assembled from multiple EST and genomic sequences. Sequence identity was determined by pairwise BLASTp alignment. (B) *ric-7* mutants are defective for acetylcholine neurotransmission. Animals become paralyzed when exposed to the acetylcholinesterase inhibitor Aldicarb due to accumulation of acetylcholine in the synaptic cleft. Paralysis in response to Aldicarb was assayed after 8 hrs. *ric-7* mutants are resistant to Aldicarb, indicating impaired acetylcholine release (n= 10-20 worms per data point). Similar results have been reported by Hao et al. [S1]. (C) In *C. elegans* GABA stimulates contraction of the enteric muscles [S2, S3]. *ric-7* mutants display reduced enteric muscle contractions following posterior body muscle contractions, and this defect was rescued by expressing RIC-7 (*oxEx233*) in the GABA neurons, 'RIC-7(+)'. n-values shown in each bar, p<0.01. (D) The active zone protein RIM (UNC-10) is normally distributed in the dorsal cord of *ric-7(n2657)* mutants. RFP is fused to the PDZ and C2A domains of RIM, which are sufficient for proper localization [S4]. The number of RIM puncta is similar between the wild type and *ric-7(n2657)* mutants (avg # of RIM puncta per 50  $\mu\text{m}$  +/- SEM, 30 and 31 images, respectively, p=0.53 two-tailed t-test). (E) A synaptic vesicle marker, the vesicular GABA transporter (vGAT/UNC-47), is normally localized in *ric-7* mutants. vGAT was tagged with GFP and inserted as a single copy. The number of vGAT::GFP puncta is normal in *ric-7* mutants (avg # of vGAT puncta per 50  $\mu\text{m}$  +/-SEM, 12 and 9 images, respectively, p=0.46 Mann-Whitney Test). (F) Electron micrographs of neuromuscular junctions in the adult ventral nerve cord revealed that *ric-7(n2657)* has normal numbers of vesicles per synapse profile (wild type: 16 synapses, 75 profiles, *ric-7(n2657)*: 15 synapses,

68 profiles). (G) The active zone protein RIM (UNC-10) is normally distributed in the dorsal cord of *ric-7(n2657)* mutants. (H) A synaptic vesicle marker, the vesicular GABA transporter (vGAT/UNC-47), is normally localized in *ric-7* mutants. (I) Dense core vesicles are distributed evenly throughout the axons of *ric-7* mutants, shown here using the neuropeptide marker FLP-3::Venus. Scale bar = 10  $\mu$ m. (J) Electron micrographs of neuromuscular junctions show synaptic vesicles (arrowheads) surrounding the dense projection (\*) for the wild type and *ric-7(n2657)*. Scale bar = 250 nm. (K) *ric-7* is expressed in neurons and head muscles. DNA 5 kb upstream of the *ric-7a* start codon through the second exon was fused to a nuclear localization signal (NLS) and GFP (left). Fluorescence was observed in most neurons in the head, as well as in the head muscles (middle), and motor neurons (right); examples of each are labeled. An asterisk marks autofluorescent gut granules. Anterior is to the left.

**Figure S2. RIC-7 and mitochondria localization, related to Figure 2.** (A)

Tagged RIC-7 (RFP::RIC-7) was made by combining the cDNA for exons 1-10 with the genomic sequence for exons 11 through the 3'UTR. The 10th intron was shortened in order to remove the coding region for F58E10.7. RFP flanked by linker sequences was inserted at the N-terminus. The construct was expressed in GABA neurons using the *unc-47* promoter. (B) When inserted as a single-copy transgene, RFP::RIC-7 is distributed diffusely in the GABA motor neuron cell body (arrowhead) and axons. Scale bar = 10  $\mu$ m. (C) Mitochondria are absent in axons of the dorsal nerve cord in *ric-7(n2657)* mutants. GABA motor neuron axons are labeled with soluble RFP and mitochondria in the GABA neurons are labelled with mito::GFP. Scale bar = 10  $\mu$ m. (D) Mito::citrine was expressed in the hypodermis under the *dpy-7* promoter. Similar structures were observed in the wild type and *ric-7* mutants. (E) Mito::citrine was expressed in the body wall muscles under the *myo-3* promoter. Muscle mitochondria form a similar network in *ric-7* mutants and the wild type. Scale bar = 5  $\mu$ m.

**Figure S3. Axon degeneration is enhanced in the absence of mitochondria, related to Figure 3.** (A) The PVQ axon remains intact in the wild type. Scale bar = 100  $\mu$ m.

(B) HSN axons spontaneously degenerate in *ric-7* mutants.

Schematic of the HSN axon in the wild type and *ric-7(zd31)* mutants. The HSN cell bodies extend a single axonal process to the nerve ring during larval development.

(C) In a wild-type animal the HSN axon is continuous and reaches into the nerve ring. (D) HSN axons were unaffected in *ric-7* young adults, yet degeneration was evident in older animals (E).

Swelling and distal degeneration was similar to that of PVQ. (F) Severed acetylcholine motor neuron axons degenerate in *ric-7* mutants but not wild-type worms.

Two acetylcholine (DB) axons were cut per animal and reimaged 24 hrs later. The presence or absence of severed axons was scored. \*\*\* $p < 0.0001$  two-tailed Fisher's Exact Test. (G) Severed ALA axons persist in the wild type but degenerate in *ric-7* mutants.

Lengths of intact ('sham') and severed ('axotomy') ALA axons 24 hrs after axotomy in wild-type worms and *ric-7* mutants. Worms with sham axotomies were mounted for surgery but the axons were not cut. ( $p < 0.0001$ , Kruskal-Wallis Test with Dunn's multiple comparisons \*\*\* $p < 0.001$  and \*\* $p < 0.01$  compared to the wild type).

(H) ALA axons were cut once near the head by laser axotomy in L2 animals and reimaged 24 hrs later. ALA axons were labelled using the *Pacr-5::GAP-43::GFP* transgene. In these images, the right side was cut in the wild type and the left in the *ric-7* worm. Arrows mark the ends of the severed axon in the wild type. Arrowheads mark the approximate location of the lesion site from the previous day. The cell bodies were killed to prevent regeneration, and an asterisk marks the former location of the cell body. Scale bar = 100  $\mu$ m. (I)

Overexpression of dominant negative DRP-1(K40S) reduces mitochondria in the distal axon and increases degeneration of GABA motor neurons. Three axons are visible immediately after axotomy. Arrowheads mark the cut sites and arrows indicate some mitochondria that have escaped into the distal axon. The worm was moving slightly after the surgery. To increase visibility these images were scaled 215% relative to the 24 hr images, both scale bars are 10  $\mu$ m. (J) After 24 hrs only the axon with escapee mitochondria is still present. Axon 1 has

completely degenerated and only two small pieces of debris remain for axon 3. Arrows indicate the location of mitochondria in Axon 2. (K) Axons were scored for their presence or absence 24 hrs after axotomy. In worms overexpressing a dominant negative form of DRP-1(K40S) only 23% of axons are still present. Of these axons, 70% contain visible mitochondria (Average % of axons present 24 hrs after axotomy +/- SEM).  $p = 0.0002$  two-tailed t-test with Welch correction for unequal variances. The wild type data is the same as in Figure 3G.

**Figure S4. The transport chimera restores mitochondria to *ric-7* axons and suppresses degeneration, related to Figure 4.** (A) Impaired mitochondrial function does not promote axon degeneration. The electron transport chain mutants *mev-1(kn1)* and *nuo-1(ua1)* do not have enhanced axon degeneration in spite of their mitochondrial dysfunction and impaired health.  $p = 0.38$  one-way ANOVA. The wild type data is the same as in Figure 3G. (B) Overexpression of the chimeric transport protein Kinesin-Tom7 restores mitochondria out into the axons of *ric-7* mutants. Scale bar = 10  $\mu\text{m}$ . (C) Axons can survive axotomy in *ric-7* mutants that are expressing Kinesin-Tom7. Two surviving axons can be seen and mitochondria are visible in the dorsal nerve cord. In the RFP-only image a mask was created over the gut autofluorescence (grey outline) so that the actual mito::RFP signal from the ventral and dorsal cords is discernable. Scale bar = 25  $\mu\text{m}$ .

**Table S1. *ric-7* mutations, related to Figure 1.**

<b>Allele</b>	<b>DNA mutation</b> (relative to <i>ric-7a</i> cDNA)	<b>Protein modification</b> (relative to RIC-7A)	<b>Mutagen</b>
<i>ox134</i>	14.6 kb deletion beginning in the 2nd intron	only amino acids 1-84 would remain	ENU
<i>zd152</i>	c148t	R50stop	ENU
<i>n2657</i>	g576a	W192stop	EMS
<i>zd31</i>	c634t	Q212stop	EMS
<i>nu447</i>	c785t, + 32 base pair deletion (nt 865-896)	A262V, + out of frame after C288 and an early stop codon at position 291	EMS

## Supplemental Experimental Procedures: Worm strains

	Strain	Genotype	Transgenes
<b>n2657</b>	MT6924	<i>ric-7(n2657) V</i>	
<b>ox134</b>	EG2355	<i>ric-7(ox134) V</i>	
<b>nu447</b>	KP7048	<i>ric-7(nu447) V</i>	
<b>zd31</b>	SK31	<i>ric-7/wly-1(zd31) V</i>	
<b>zd152</b>	SK152	<i>ric-7/wly-1(zd152) V</i>	
<b>Pric-7::GFP</b>	EG1702	<i>lin-15(n765ts) X; oxEx174</i>	<i>Pric-7a::NLS::GFP, lin-15(+)</i>
<b>RIC-7::GFP</b>	EG1474	<i>ric-7(n2657) V; lin-15(n765ts) X; oxEx233</i>	<i>Punc-47::RIC-7::GFP, lin-15(+)</i>
<b>PCR rescue</b>	EG2298	<i>ric-7(n2657) V; lin-15(n765ts) X</i>	18kb PCR product, <i>lin-15(+)</i>
<b>RIM wild type</b>	EG7001	<i>lin-15(n765ts) V; oxEx1637</i>	<i>Punc-47::RIM_C2APDZ::RFP, Pmyo-2::GFP, lin-15(+)</i>
<b>RIM n2657</b>	EG7000	<i>ric-7(n2657) V; lin-15(n765ts) X; oxEx1636</i>	<i>Punc-47::RIM_C2APDZ::RFP, Pmyo-2::GFP, lin-15(+)</i>
<b>vGAT wild type</b>	EG5717	<i>unc-119(ed3) III; oxSi36 IV</i>	<i>Punc-47::unc-47+GFP(E144), CB unc-119(+)</i>
<b>vGAT n2657</b>	EG5787	<i>oxSi36 IV; ric-7(n2657) V</i>	<i>Punc-47::unc-47+GFP(E144), CB unc-119(+)</i>
<b>FLP-3 wild type</b>	KG1645	<i>cels61 II</i>	<i>Punc-129::flp-3::Venus, Punc-129::mCherry::snb-1, Pttx-3::mCherry</i>
<b>FLP-3 n2657</b>	EG6336	<i>ric-7(n2657) V; cels61 II</i>	<i>Punc-129::flp-3::Venus, Punc-129::mCherry::snb-1, Pttx-3::mCherry</i>
<b>RFP::RIC-7</b>	EG6793	<i>ric-7(n2657) V; lin-15(n765ts) X; oxEx1598</i>	<i>Punc-47::RFP_ric-7AcDNA_3'minigene, Punc-47::Tom20::GFP, lin-15(+)</i>
<b>mito::GFP wild type</b>	EG5043	<i>lin-15(n765ts) X; oxEx1182</i>	<i>Punc-47::Tom20::GFP, Pmyo-2::GFP, lin-15(+)</i>
<b>mito::GFP n2657</b>	EG6496	<i>ric-7(n2657) V; lin-15(n765ts) X; oxEx1182</i>	<i>Punc-47::Tom20::GFP, Pmyo-2::GFP, lin-15(+)</i>
<b>mito::GFP ox134</b>	EG7308	<i>ric-7(ox134) V; lin-15(n765ts) X; oxEx1772</i>	<i>Punc-47::Tom20::GFP, Pmyo-2::GFP, lin-15(+)</i>
<b>Axon::RFP mito::GFP</b>	EG6531	<i>oxIs608; oxEx1182</i>	<i>Punc-47::mCherry; Punc-47::Tom20::GFP, Pmyo-2::GFP</i>
<b>Axon::RFP mito::GFP</b>	EG7161	<i>ric-7(n2657) V; lin-15(n765ts) X; oxEx1720</i>	<i>Punc-47::mCherry, Punc-47::Tom20::GFP, lin-15(+)</i>
<b>PVQ axon wild type</b>	PY1058	<i>oyIs14 V</i>	<i>Psra-6::GFP</i>
<b>PVQ axon zd152</b>	SK5175	<i>ric-7/wly-1(zd152) oyIs14 V</i>	<i>Psra-6::GFP</i>
<b>ALA:GFP wild type</b>	EG1399	<i>lin-15(n765ts) X; oxEx81</i>	<i>Pacr-5::GAP43::GFP, lin-15(+)</i>
<b>ALA:GFP n2657</b>	EG1968	<i>ric-7(n2657) V; lin-15(n765ts) X; oxEx81</i>	<i>Pacr-5::GAP43::GFP, lin-15(+)</i>
<b>ALA:GFP ox134</b>	EG1967	<i>ric-7(ox134) V; lin-15(n765ts) X; oxEx81</i>	<i>Pacr-5::GAP43::GFP, lin-15(+)</i>
<b>ALA:GFP mito::RFP</b>	EG6863	<i>oxIs609; oxEx1606</i>	<i>Pacr-5::GAP43::GFP, lin-15(+); Pida-1::Tom20::RFP</i>
<b>GABA cuts wild type</b>	EG1285	<i>lin-15(n765ts) oxIs12 X</i>	<i>Punc-47::GFP, lin-15(+)</i>
<b>GABA cuts n2657</b>	EG1960	<i>ric-7(n2657) V; lin-15(n765ts) oxIs12 X</i>	<i>Punc-47::GFP, lin-15(+)</i>
<b>RFP::RIC-7 single copy</b>	EG6753	<i>unc-119(ed3) III; oxSi451 II</i>	<i>Punc-47::RFP::ric-7AcDNA_3'minigene, Cb-unc-119(+)</i>
<b>Hypodermis mito WT</b>	EG6463	<i>lin-15(n765ts) X; oxEx1541</i>	<i>Pdpy-7::Tom20::citrine, lin-15(+)</i>
<b>Hypodermis mito n2657</b>	EG6611	<i>ric-7(n2657) V; lin-15(n765ts) X; oxEx1541</i>	<i>Pdpy-7::Tom20::citrine, lin-15(+)</i>
<b>Muscle mito wild type</b>	EG5515	<i>lin-15(n765ts) X; oxEx1329</i>	<i>Pmyo-3::Tom20::citrine, lin-15(+)</i>
<b>Muscle mito n2657</b>	EG6859	<i>ric-7(n2657) V; lin-15(n765ts) X; oxEx1329</i>	<i>Pmyo-3::Tom20::citrine, lin-15(+)</i>
<b>HSN ric-7(zd31)</b>	SK5249	<i>zdlIs13 IV; ric-7/wly-1(zd31) V</i>	<i>tph-1::gfp</i>
<b>kinesin-1 mito::GFP</b>	EG6615	<i>unc-116(rh24sb79) III; oxEx1182</i>	<i>Punc-47::Tom20::GFP, Pmyo-2::GFP, lin-15(+)</i>

<b>kinesin-3 mito::GFP</b>	EG8300	<i>unc-104(e1265) II; oxEx1182</i>	<i>Punc-47::Tom20::GFP, Pmyo-2::GFP, lin-15(+)</i>
<b>kinesin-1 axotomy</b>	MJB1280	<i>unc-116(rh24sb79) III; oxIs12 X</i>	<i>Punc-47::GFP, lin-15(+)</i>
<b>kinesin-3 axotomy</b>	MJB1281	<i>unc-104(e1265) II; oxIs12 X</i>	<i>Punc-47::GFP, lin-15(+)</i>
<b>DRP-1(K40S)</b>	EG8125	<i>oxIs12 X; oxEx1974</i>	<i>Punc-47::DRP-1(K40S), Punc-47::Tom20::mCherry, Pmyo-2::mCherry, lin-15(+)</i>
<b>Kinesin::Tom7</b>	EG8301	<i>oxIs12 X; oxEx1973</i>	<i>Punc-47::unc-116_GFP::tomm-7, Punc-47::Tom20::mCherry, Pmyo-2::mCherry, lin-15(+)</i>
<b>Kinesin::Tom7 <i>ric-7(n2657)</i></b>	EG8124	<i>ric-7(n2657) V; lin-15(n765ts) oxIs12 X; oxEx1973</i>	<i>Punc-47::unc-116_GFP::tomm-7, Punc-47::Tom20::mCherry, Pmyo-2::mCherry, lin-15(+)</i>
<b>mev-1</b>	EG8302	<i>mev-1(kn1) III; oxIs12 X</i>	<i>Punc-47::GFP, lin-15(+)</i>
<b>nuo-1</b>	EG8303	<i>nuo-1(ua1)/mln1[dpy-10(e128) mls14] II; oxIs12 X</i>	<i>Punc-47::GFP, lin-15(+)</i>

## SUPPLEMENTAL EXPERIMENTAL PROCEDURES

### Strains

Animals were maintained on *E. coli* OP50-seeded NGM plates according to standard methods. See the table above for a complete list of strains.

### Cloning of *ric-7*

Three *ric-7* alleles were isolated from three behavioral screens for neurotransmission defective mutants: defecation defective, aldicarb resistance [S1] and shrinker behavior, *n2657*, *nu447* and *ox134*, respectively. The *ric-7* reference allele *n2657* was isolated in a screen for excitatory GABA neurotransmission defective mutants. Wild-type hermaphrodites were treated with ethyl methanesulfonate (EMS), and F2 progeny were screened for animals exhibiting a constipated phenotype. Two alleles (*zd31*, *zd152*) were recovered from a screen for mutants with defects in growth or morphology of the PVQ axons (see Clark & Chiu [S5] for details). In brief, *sra-6::gfp(oyIs14)* animals were treated with EMS or N-ethyl-N-nitrosourea (ENU), and F2 progeny that exhibited behavioral defects were picked. F3 progeny were then examined using epifluorescence microscopy to find mutants with PVQ axonal defects. The alleles *zd31* and *zd152* exhibited discontinuous blebbing and truncation of the PVQ axons and the gene was named *wly-1* (wallerian-like decay). *wly-1* and *ric-7* were independently cloned and later established to be the same gene. Because the gene name *ric-7* is published, we use the name *ric-7* as well.

The reference allele *n2657* was mapped between *lin-25* and *unc-76* on chromosome V. Three-factor mapping placed *ric-7* to the left of *him-5* (Figure 1A). Cosmid F58E10 rescued the Aldicarb-resistance phenotype of *ric-7* mutants by germline transformation. F58E10 contains 11 predicted genes. Using PCR and germline rescue experiments, we localized the rescuing activity of F58E10 to an 18 kilobase fragment that contains two hypothetical genes, F58E10.1 and F58E10.7 (Figure 1A). A similar series of mapping and rescue experiments identified F58E10.1 as the gene *wly-1*. To ascertain which of the two candidate genes represents *ric-7/wly-1*, we identified the molecular lesions associated with the five mutant alleles. All alleles contain mutations in F58E10.1 exons (Figure 1B). Mutations are summarized in Supplemental Table 1.

**Gene Structure and Protein.** The *ric-7* coding region is contained in 13 exons dispersed over 15 kb (WBGene00010259, [www.wormbase.org](http://www.wormbase.org)). We sequenced the full-length *ric-7* cDNA clone yk14h10 (gift from Yuji Kohara, Japan) to confirm the predicted gene structure. The *ric-7* cDNA contains 2085 bases of coding sequence, 86 bp of 5' UTR and 378 bp of 3' UTR. Analysis of *ric-7* cDNAs indicates that *ric-7* encodes two splice forms that differ in their first exon: RIC-7A (694 aa) and RIC-7B (709 aa).

To investigate the function of RIC-7 we sought possible homologous sequences. Blast searches of the full-length protein with sequence databases failed to identify homologs in species outside of nematodes. Even within nematodes, RIC-7 sequences appear to have diverged rapidly (Figure S1A). The RIC-7 amino acid sequence does not contain any obvious protein domains.

Gene expression analysis indicates that *ric-7a* is expressed primarily in neurons and a few muscles. We generated a reporter containing genomic sequence from 5 kb upstream of the *ric-7a* ATG through to the second exon fused to a nuclear localization signal (NLS) and GFP. GFP was detected primarily in neurons as well as in the head muscle cells (Figure S3A). Despite the presence of an NLS, GFP expression appears to be cytosolic.

## **Molecular Biology**

Most plasmids were made using the Invitrogen multisite Gateway cloning technique. We created the mitochondrial marker by fusing GFP to the mitochondrial

targeting sequence (first 54 amino acids) of the translocase of outer mitochondrial membrane (Tom20, encoded by *tomm-20*) [S6]. RIM localization was determined by fusing RFP to the C2A and PDZ domains of UNC-10. These two domains are sufficient to localize the RIM fragment to the dense projection [S7]. The synaptic vesicle marker was constructed by inserting GFP between E144 and N145 of UNC-47. The construct was inserted into the worm genome as a single copy using the MosSCI technique [S8]. The ALA:GFP transgene (*oxEx81*) encodes a membrane-bound GFP (40 aa myristoylation sequence of GAP43::GFP) and is expressed under the *acr-5* promoter [S9]. *oxIs609* was generated by X-ray integration of *oxEx81*.

The constructs for tagging RIC-7 with RFP were made by combining the cDNA for exons 1-10 (Gateway [1-2] vector) with the genomic sequence for exons 11 through the 3'UTR (Gateway [2-3] vector). The third recombination site attB2 is embedded within the 10th intron, which was shortened to remove the coding region for F58E10.7. This hybrid construct expressed under the *unc-47* promoter rescued mitochondrial distribution in the GABA motor neurons. RFP flanked by linker sequences was inserted into the base constructs at five different locations; N-terminus, C-terminus, H104, E332 and Q440. All three internal tags yielded modest to poor rescue of mitochondrial distribution. The N-terminal tag was the only transgene that was visible when integrated at single copy. The A splice form was used because it provided better rescue of the mitochondrial localization defect than the B form did (data not shown).

The mitochondria transport chimera construct (Kinesin-Tom7) contains the following elements in order from 5' to 3': the *unc-47* promoter (1,254 bp), the cDNA for *unc-116* (2,448 bp), linker sequence (36 bp), GFP with syntons (864 bp), att recombination site + 2<sup>nd</sup> linker (63 bp), the genomic sequence of *tomm-7* (437 bp), and the *let-858* 3' UTR (439 bp). The *unc-116* cDNA through GFP are in a [1-2] Gateway vector and the second linker through the 3'UTR are in a [2-3] Gateway vector.

## **Behavioral Assays**

In *C. elegans* defecation is a programmed behavior that occurs every 45-50 seconds. The defecation cycle is initiated by a posterior body wall muscle contraction (pBoc) and completed with an enteric muscle contraction (Emc). The Emc requires nervous system function and the excitatory action of the neurotransmitter GABA [S2,

S3, S10]. The defecation cycle of young adults from each strain were scored as described previously [S11]. Briefly, the number of pBocs followed by an Emc were quantified. For Figure 4F each worm was assayed for at least 6 cycles.

Aldicarb sensitivity was assayed as previously described [S12]. Unless otherwise stated, Aldicarb was added to NGM plates at the final concentrations: 0.01, 0.02, 0.04, 0.09, 0.18, 0.35, 0.70, 1.4 mM. Ten to 20 young adults from each strain were placed on a plate at each Aldicarb concentration, incubated at 20°C for 8 hours and then scored.

### **Electron Microscopy**

Adult nematodes were prepared for transmission electron microscopy as previously described [S13]. Specimens were fixed in 0.8% glutaraldehyde, 0.7% osmium tetroxide in 0.1 M cacodylate for 2 hr and then washed in buffer. Next, the animals' heads and tails were removed, the tissue postfixed in 2% osmium tetroxide in 0.1 M cacodylate overnight at 4°C then washed extensively in water. 117 specimens were then stained *en bloc* in 1% uranyl acetate, dehydrated with ethanol, passed through propylene oxide and embedded in epoxy resin. Ribbons of ultrathin (~33 nm) sections were imaged.

### **Imaging**

Worms were immobilized in either 10 mM muscimol or 25 mM sodium azide on 3% agarose pads. Images were acquired on a Pascal LSM5 confocal microscope (Zeiss) with a 63x 1.4NA oil objective. Dorsal and ventral cord images were taken with the cord facing toward the objective. Three Z-stacks were acquired from each worm, 16.81  $\mu\text{m}$  by 96.84  $\mu\text{m}$  with a 1.5 zoom factor. The total number of fluorescent puncta was quantified from maximum intensity projections using the Cell Counter ImageJ plugin. Images were blinded by assigning each a random 5-digit number generated in Excel. The data are presented as the average number of puncta per 50  $\mu\text{m}$ .

Images of the RFP::*RIC-7* single copy insert (Figure S2B) were acquired using a Nikon spinning disc confocal with a Photometrics Cascade II EMCCD camera, generously made available by the laboratory of V. Maricq. A single focal plane was imaged with a 300 ms exposure time. The signal is very dim, so 20 frames were averaged to enhance the signal-to-noise ratio.

## Laser Axotomy

L2 worms were immobilized as described above. Axons containing GFP were cut using 1) a pulsing 810 nm light from a Ti:Sapphire laser (Mira900, Coherent) assembled on a LSM510 Meta confocal microscope (Zeiss) and focused through a 63x 1.4NA objective or 2) a pulsing 355 nm laser (FTSS355-Q3, CryLaS GmbH, Germany) assembled on a Nikon D-Eclipse C1, 90i confocal microscope with a Nikon 40x 1.3NA objective. The ALA neuron has a single cell body in the head of the worm (dorsal to the posterior bulb of the pharynx) and extends two axons along the length of the worm at the right and left midline. In all experiments either the right or left axon was cut and the same side of the worm was imaged on the following day. After the axons were cut, the laser was used to kill the cell bodies, which would otherwise regenerate new axons that obscure the degeneration analysis. Images were acquired immediately after cutting. Worms were then recovered from the agarose pad and placed on bacterial NGM plates for 24 +/- 4 hrs. Images were acquired on the Pascal confocal (Zeiss) on the following day. For the *ric-7* experiments (Figure 5A,B) the ALA axon was cut once in the anterior of the worm behind the head, and then the cell body was killed. Images from the following day were analyzed in ImageJ by tracing the axon segment to measure its length.

For the wild-type experiments (Figure 5D-F), the ALA axon was cut into multiple pieces proceeding anterior to posterior, and then the cell body was killed. The most anterior and posterior axon pieces were not included in the analysis, since the head and tail ganglia make it impossible to determine the presence or absence of mitochondria in these segments. On average there were four axon segments per worm, and 61% of segments contained at least one mitochondrion. For each worm the images from both days were compared side-by-side to determine which segments were still present. Each segment was also scored for the presence or absence of mitochondria at both time points.

The GABA and acetylcholine motor neuron commissures were cut once just below the midline of the worm. The cell bodies were then killed to prevent regeneration. Four to five VD/DD or two DB commissures were cut per worm; the transgenes *oxIs12* and *oxEx81* were used, respectively. The worms were imaged again 24 hrs later and

the number of commissures still present was quantified. The GFP in the GABA motor neuron experiments is soluble and on occasion would leak out of the commissures immediately following the injury. Images were acquired post-axotomy and only commissures that were still visible were included in the 24 hr analysis.

## Statistics

In most cases non-parametric tests were used; the Kruskal-Wallis for multiple comparisons and the Fisher's Exact test for two-sample data sets. The data sets did not meet the requirements for parametric tests for the following reasons. The mitochondria distribution and enteric muscle contraction data sets did not pass the equal variance test. The degeneration data sets are not normally distributed because the *ric-7* data is consistently at zero. All statistics were performed with the GraphPad InStat software.

## SUPPLEMENTAL REFERENCES

- S1. Hao, Y., Hu, Z., Sieburth, D., and Kaplan, J. M. (2012). RIC-7 promotes neuropeptide secretion. *PLoS Genet.* *8*, e1002464.
- S2. Liu, D. W., and Thomas, J. H. (1994). Regulation of a periodic motor program in *C. elegans*. *J. Neurosci.* *14*, 1953–1962.
- S3. McIntire, S. L., Jorgensen, E., Kaplan, J., and Horvitz, H. R. (1993). The GABAergic nervous system of *Caenorhabditis elegans*. *Nature* *364*, 337–341.
- S4. Otsuga, D., Keegan, B.R., Brisch, E., Thatcher, J.W., Hermann, G.J., Bleazard, W., and Shaw, J.M. (1998). The dynamin-related GTPase, Dnm1p, controls mitochondrial morphology in yeast. *J. Cell Biol.* *143*, 333-349.
- S5. Clark, S. G., and Chiu, C. (2003). *C. elegans* ZAG-1, a Zn-finger-homeodomain protein, regulates axonal development and neuronal differentiation. *Development* *130*, 3781–3794.
- S6. Watanabe, S., Punge, A., Hollopeter, G., Willig, K. I., Hobson, R. J., Davis, M. W.,

- Hell, S. W., and Jorgensen, E. M. (2011). Protein localization in electron micrographs using fluorescence nanoscopy. *Nat. Meth.* **8**, 80–84.
- S7. Deken, S. L., Vincent, R., Hadwiger, G., Liu, Q., Wang, Z.-W., and Nonet, M. L. (2005). Redundant localization mechanisms of RIM and ELKS in *Caenorhabditis elegans*. *J. Neurosci.* **25**, 5975–5983.
- S8. Frøkjaer-Jensen, C., Davis, M. W., Hopkins, C. E., Newman, B. J., Thummel, J. M., Olesen, S.-P., Grunnet, M., and Jorgensen, E. M. (2008). Single-copy insertion of transgenes in *Caenorhabditis elegans*. *Nat. Genet.* **40**, 1375–1383.
- S9. Knobel, K. M., Davis, W. S., Jorgensen, E. M., and Bastiani, M. J. (2001). UNC-119 suppresses axon branching in *C. elegans*. *Development* **128**, 4079–92.
- S10. McIntire, S. L., Jorgensen, E., and Horvitz, H. R. (1993). Genes required for GABA function in *Caenorhabditis elegans*. *Nature* **364**, 334–337.
- S11. Thomas, J. H. (1990). Genetic analysis of defecation in *Caenorhabditis elegans*. *Genetics* **124**, 855–872.
- S12. Nguyen, M., Alfonso, A., Johnson, C. D., and Rand, J. B. (1995). *Caenorhabditis elegans* mutants resistant to inhibitors of acetylcholinesterase. *Genetics* **140**, 527–535.
- S13. Jorgensen, E. M., Hartweg, E., Schuske, K., Nonet, M. L., Jin, Y., and Horvitz, H. R. (1995). Defective recycling of synaptic vesicles in synaptotagmin mutants of *Caenorhabditis elegans*. *Nature* **378**, 196–199.